

$$\begin{aligned}
& -m^2 \frac{\partial}{\partial x^1} \left[\frac{\overline{\rho J_\xi}}{m^2} \left(K^{11} \frac{\partial q_i}{\partial x^1} \right) \right] - m^2 \frac{\partial}{\partial x^2} \left[\frac{\overline{\rho J_\xi}}{m^2} \left(K^{22} \frac{\partial q_i}{\partial x^2} \right) \right] - \frac{\partial}{\partial x^3} \left[\overline{\rho J_\xi} \left(K^{33} \frac{\partial q_i}{\partial x^3} \right) \right] \\
& \qquad \qquad \qquad \text{d)} \qquad \text{e)} \\
& -m^2 \frac{\partial}{\partial x^1} \left[\frac{\overline{\rho J_\xi}}{m^2} \left(K^{13} \frac{\partial q_i}{\partial x^3} \right) \right] - m^2 \frac{\partial}{\partial x^2} \left[\frac{\overline{\rho J_\xi}}{m^2} \left(K^{23} \frac{\partial q_i}{\partial x^3} \right) \right] - \frac{\partial}{\partial x^3} \left[\overline{\rho J_\xi} \left(K^{31} \frac{\partial q_i}{\partial x^1} + K^{32} \frac{\partial q_i}{\partial x^2} \right) \right] \\
& \qquad \qquad \qquad \text{f)} \qquad \text{g)} \\
& = J_\xi R_{\varphi_i} (\overline{\varphi_1}, \dots, \overline{\varphi_l}) + J_\xi Q_{\varphi_i} + \frac{\partial (\overline{\varphi_i J_\xi})}{\partial t} \Big|_{cld} + \frac{\partial (\overline{\varphi_i J_\xi})}{\partial t} \Big|_{aero} + \frac{\partial (\overline{\varphi_i J_\xi})}{\partial t} \Big|_{ping} \\
& \qquad \qquad \qquad \text{h)} \qquad \qquad \text{i)} \qquad \text{j)} \qquad \qquad \text{k)} \qquad \qquad \text{l)} \qquad \qquad \qquad \qquad \qquad \qquad \qquad \text{(1)}
\end{aligned}$$

The terms in equation (1) are summarized as follows: a) time rate of change of pollutant concentration; b) horizontal advection; c) vertical advection; d) horizontal eddy diffusion (diagonal term); e) vertical eddy diffusion (diagonal term); f) off-diagonal horizontal diffusion; g) off-diagonal vertical diffusion; h) production or loss from chemical reactions; i) emissions; j) cloud mixing and aqueous-phase chemical production or loss; k) aerosol process and l) plume-in-grid process where φ_i is the trace species concentration in density units (e.g., kgm^{-3}), J_ξ is the vertical Jacobian of the terrain-influenced coordinate ξ , m is the map scale factor, V_s is the vertical and horizontal wind components in the generalized coordinates, q_i is the species mass mixing ration, K are the diagonal components of the eddy diffusivity tensor in the generalized coordinates, ρ is the density of the air. The dry deposition process can be included in the vertical diffusion process as a flux boundary condition at the bottom of the model layer. The numerical solution of the Equation (1) is a so-called air quality dispersion model which is referred in the present contribution.

2. EXPERIMENT

During the summer 2003 (5-10 August), several air quality monitoring stations in Europe reached quite high values ($200 - 300 \mu\text{gm}^{-3}$). During this period of time the ozone concentrations increase continuously and the central and western part of Europe experienced very high temperatures (higher than 40 C in surface) (see Fig. 1) because an stagnation of hot air coming from Africa. The high pressures were kept during the entire episode. We have implemented MM5 (PSU/NCAR) (Grell et al., 1994) and the WRF (Weather Research and Forecasting) model (Skamarock (2004,2006)) to produce initial meteorological 3D fields to be used as input for CMAQ model (Byun et al., 1998).

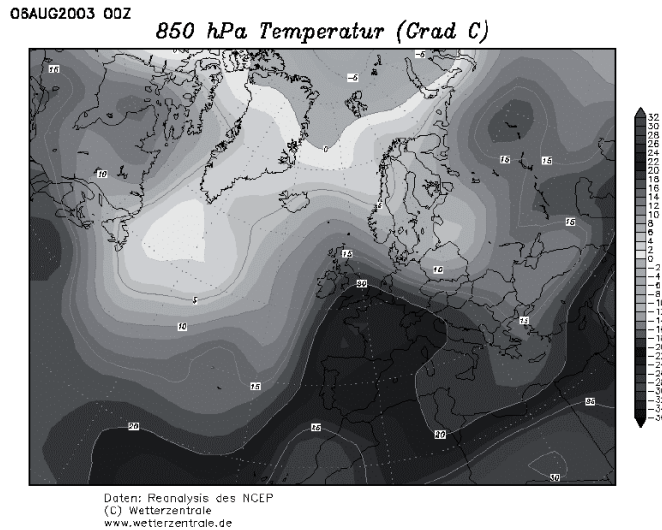


Figure 1. Re-analysis from NCEP for August, 6, 2003 00:00 GMT. A strong air stagnation is observed in the Central and Western part of Europe with high temperatures at 850 hPa.

The domain is set with 182x182 grid cells with 27 km spatial resolution with 23 vertical layers. The Lambert Conformal projection is used. We use 24 USGS land use categories. Figure 2 shows the domain. MM5 and WRF models provide input data for the so-called MCIP module which converts meteorological data in terms to be used by CMAQ dispersion model. See Figure 2. Both modelling systems were run in the super-computer MAGERIT with 1200 IBM eserver Blade Center JS20 and each processor is Power PC with 2,2 Ghz and 4 Gb RAM memory. For the simulations performed during August 5-10, 2003 (120 hours) we used 32 processors and MM5 took 241 CPU minutes to perform the full simulation, WRF required 560m minutes and CMAQ used 120 minutes when linked to MM5 and 125 minutes when linked with WRF. Figure 3 shows the CPU performance of CMAQ with 30 km spatial resolution over European domain with different amounts of processors. See how the optimal number for this particular architecture is found on 64 processors and for 128 and 256 processors, the CPU time is higher.

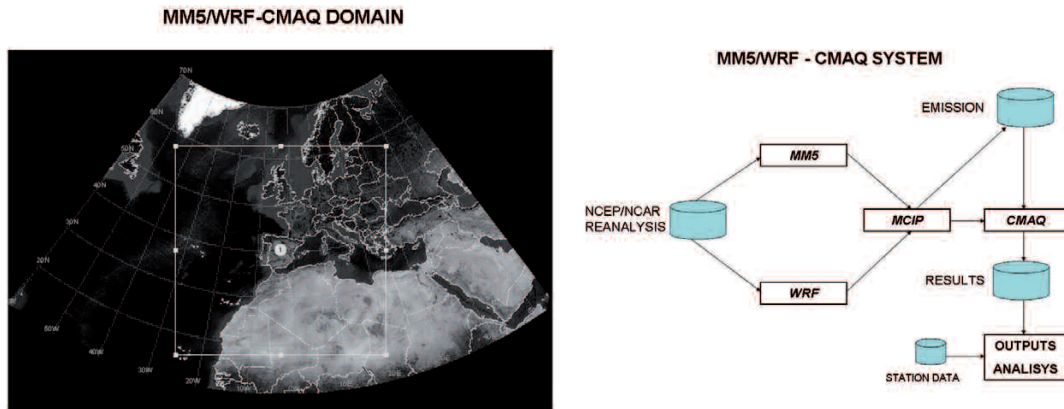


Figure 2. Domain of the experiment. Scheme of the different modules used for this experiment.

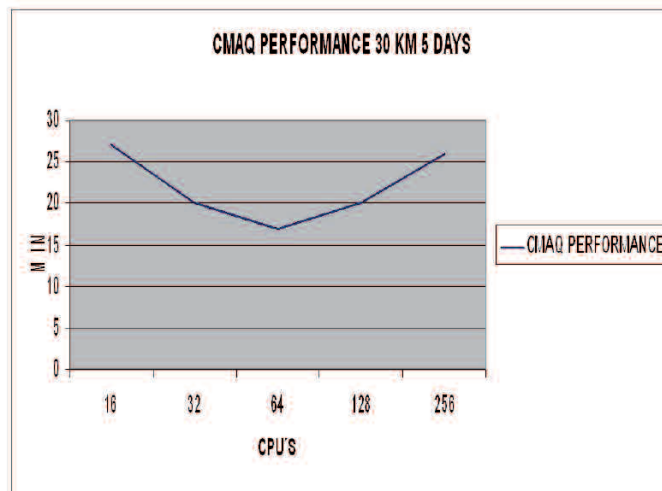


Figure 3. CMAQ CPU performance in IBM JS20 Blade cluster in MAGERIT (UPM, Madrid, Spain).

NCEP (NNRP DS090 with T62 spatial resolution which is equivalent to 209 km) re-analysis data is used to initialize the meteorological fields in CMAQ and WRF models. Re-analysis data has 28 vertical sigma levels which have been interpolated to the 23 vertical sigma levels used in this experiment by using the NCAR Command Language tool, every 6 hours during the 120 hours experiment. The MM5 configuration is set to: a) Cumulus-Parameterization is done with Kain-Fritsch 2; b) PBL and diffusion is set with MRF-PBL scheme; c) The explicit moisture scheme is done with Schultz microphysics; d) The radiation scheme is the so-called cloud-radiation and e) The surface scheme is done with the Noah Land-Surface model. The WRF model configuration is set as follows: a) Cumulus-Parameterization is set with the Grell-Devenyi Ensemble Scheme; b) The PBL scheme and diffusion is done with YSU PBL scheme; c) The explicit moisture scheme is done with the WSM (WRF single-moment) 5-class microphysics method; d) The radiation scheme is done with the RRTM-Dudhia radiation method and e) The surface scheme is performed with the Noah Land-Surface model. The CMAQ model configuration is as follows: a) Advection scheme: global mass-conserving scheme (Yamartino); b) Vertical diffusion: Asymmetric Convective

Model (ACM2); c) CB05 chemical mechanism (Yarwood et al. 2005); d) Euler Backezard solver (EBI solver); e) CMAQ aerosol: The third generation modal CMAQ aerosol model and f) The CMAQ aqueous chemistry scheme. The modal approach uses the Aiken, accumulation and coarse modes. The initial and boundary condition for CMAQ are set by using the so-called “clean profile”. TNO –UBA emission data is used with ¼ x 1/8 degree spatial resolution and EURODELTA time profiles. VOC splitting is done with SPECIATE 4.0 for 1594 compounds and VOC-to-TOG conversion factors. For Africa area we have used the EMIMO (San José et al., 1997, 1999, 2000) model based on the EDGAR global emission inventory.

3. RESULTS

The results show that the night nitrogen dioxide values are not well captured (underestimated) by both models and the evening values are overestimated. Figure 4 shows a comparison between averaged over the 2694 European stations (AIRBASE) used for the comparison between observed and modelled data. The ozone analysis shows that WRF-CMAQ ozone values increase during the full period (120 hours) but the MM5-CMAQ values increase smoothly and compare better with the averaged observed ozone concentrations.

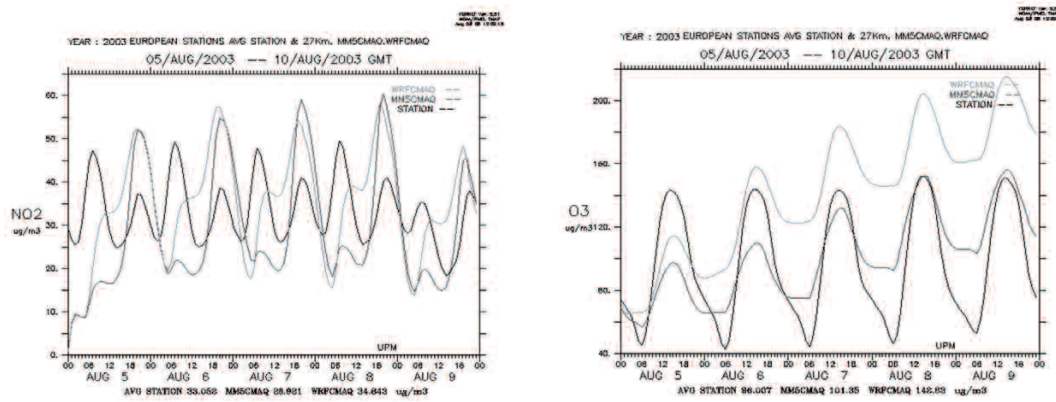


Figure 4. Comparison between averaged ozone and NO2 concentrations for the 2694 European monitoring stations in European AIRBASE and the modelled results with MM5-CMAQ and WRF-CMAQ for the 120 hours period.

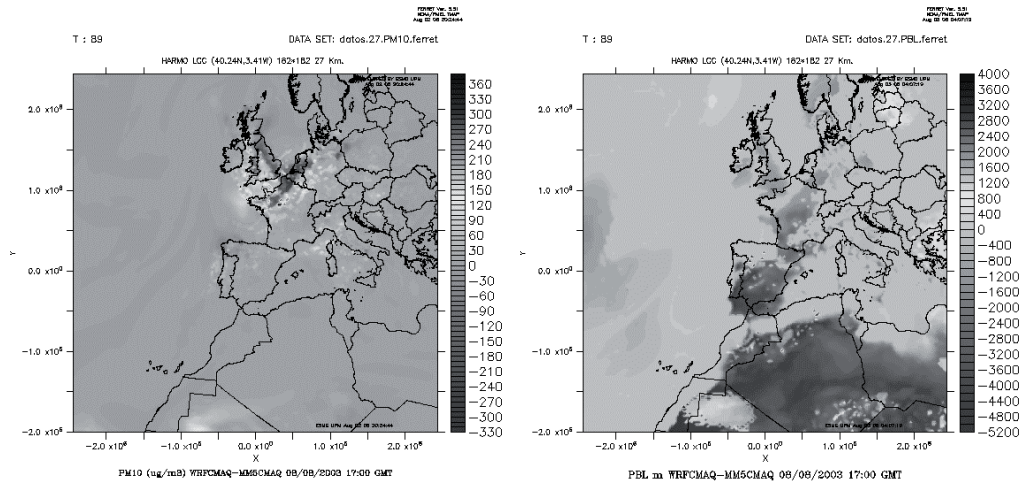


Figure 5. Differences between WRF-CMAQ and MM5-CMAQ simulations for PM10 concentrations and PBL height for August 8, 2003 17:00 GMT. It is seen that in MM5-CMAQ presents much higher concentrations than WRF-CMAQ in UK and north parts of France, Belgium and The Netherlands and also much lower concentrations in the same area. The PBL heights are much higher for MM5-CMAQ than WRF-CMAQ for North of Africa and South of Spain areas.

The differences shown in Figure 5 for PBL heights and PM10 concentrations show that MM5 and WRF meteorological results are substantially different and as a consequence the pollution concentrations are also substantially different. The Figure 6 shows similar results for Monin-Obukhov length and surface temperature values. Important differences in the meteorology lead to substantial differences in the pollution concentration values.

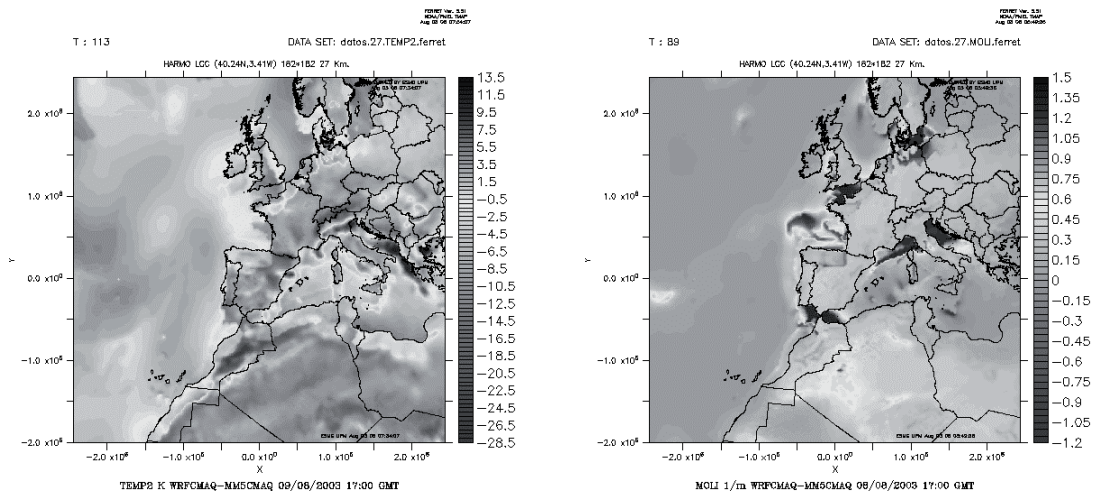


Figure 6. Differences between WRF-CMAQ and MM5-CMAQ simulations for surface temperature and inverse of Monin-Obukhov length for August, 8, 2003 17:00 GMT. It is seen that the MM5-CMAQ presents much lower unstable conditions than WRF-CMAQ in Gibraltar area, Calais straight, Baltic sea, Adriatic sea and north parts of the Mediterranean. The temperature differences shows that WRF is obtaining higher temperatures than MM5 in the ocean and sea areas but lower in the continental areas and much lower in high mountain areas.

REFERENCES

- Baklanov, A., A. Rasmussen, B. Fay, E. Berge and S. Finardi, 2002: Potential and Shortcomings of Numerical Weather Prediction Models in Providing Meteorological Data for Urban Air Pollution Forecasting. *Water, Air and Soil Poll.: Focus*, **2**(5-6), 43-60.
- Byun, D.W., J. Young, G. Gipson, J. Godowitch, F. Binkowski, S. Roselle, B. Benjey, J. Pleim, J. Ching, J. Novak, C. Coats, T. Odman, A. Hanna, K. Alapaty, R. Mathur, J. McHenry, U. Shankar, S. Fine, A. XDiu and C. Jang, 1998: Description of the Models-3 Community Multiscale Air Quality (CMAQ) model. *Proceedings of the American meteorological Society, 78th Annual Meeting*, Phoenix, AZ, Jan. 11-16, 1998.
- Etling, D. and R.A. Brown, 1993: Roll vortices in the planetary boundary layer: A review. *Boundary-Layer Meteorol.*, **65**, 215-248.
- Grell, GA, J. Dudhia, DR. Stauffer, 1994: A description of the fifth-generation Penn state/NCAR mesoscale model (MM5). *NCAR/TN- 398+ STR. NCAR Technical Note*.
- Press, W. H, S. A. Teukolsky, W. T. Vetterling and B. P. Flannery, 1988: *Numerical recipes in C*, 2nd Edition, Cambridge University Press, UK, 350 pp.
- San José, R., J.F. Prieto, J. Martín, L. Delgado, E. Jiménez and R.M. González, 1997: Integrated environmental monitoring, forecasting and warning systems in metropolitan areas (EMMA): Madrid application. *Computational Mechanics Publications*. ISBN: 1-85312-461-3.
- San José, R., M.A. Rodríguez, A. Pelechano and R.M. González, 1999: Sensitivity study of dry deposition fluxes. In *Measuring and Modelling investigation of environmental processes*. Ed. R. San José. WITpress. ISBN: 1-85312566; ISSN: 1460-1427. 205-246.
- San José, R., M.A. Rodríguez, I. Salas and R.M. González, 2000: On the use of MRF/AVN global information to improve the operational air quality model OPANA. *Environmental Monitoring and Assessment*, **65**, 477-484.
- Skamarock, W. C., 2004: Evaluating Mesoscale NWP Models Using Kinetic Energy Spectra. *Mon. Wea., Rev.*, **132**, 3019-3032.
- Skamarock, W. C., 2006: Positive-Definite and Montonic Limiters for Unrestricted-Timestep Transport Schemes. *Mon. Wea. Rev.*, **134**, 2241-2250.
- Yarwood, G., S. Rao, M. Yocke, and G. Whitten, 2005: Updates to the carbon bond chemical mechanism: CB05. Final report to the U.S. EPA, RT-0400675.